X-RAY ABSORPTION AND SCATTERING ISSUES FOR ROD-PINCH RADIOGRAPHIC SOURCES*

David Mosher[+], David D. Hinshelwood, Gerald Cooperstein, Brett Huhman, and Raymond J. Allen
Plasma Physics Division, Naval Research Lab., 4555 Overlook Ave. SW, Wash. DC 20375, USA

Stephen S. Lutz and Michael J. Berninger
National Security Technologies, 5520 Ekwill Street, Santa Barbara, CA 93111, USA

Bryan V. Oliver
Advanced Radiographic Tech., MS 1195, Sandia National Labs, Albuquerque, NM 87185, USA

Salvador Portillo
Ktech Corporation, 10800 Gibson SE, Albuquerque, NM 87123 USA

Todd Haines
Physics Division, P-23, Los Alamos National Laboratory, Los Alamos, NM 87545, USA

Abstract

During the past decade, the rod-pinch diode has been used extensively for high-brightness, megavolt x-ray radiography. Success of the rod pinch derives from its small radiographic spot size for a range of driving voltages and x-ray spectra. Here, we examine two experimentally observed and more subtle phenomena that may impact radiographic performance for some systems: flat-field nonuniformity in the image plane due to x-ray absorption in the rod, and weak, large-scale structures around radiographic features due to cathode-scattered x-rays. X-ray imaging data from Cygnus and HRS are analyzed by the ITS Monte Carlo codes to determine if these phenomena are significant for Cygnus.

I. INTRODUCTION

During the past decade, the megavolt pulsed-power-driven rod-pinch source has been used extensively for high-brightness x-ray radiography [1, 2]. For this application, a mm-or-less diameter tungsten rod anode extends through a washer-shaped cathode, and magnetic forces drive the electron beam emitted from the cathode to a pinch onto the tapered rod tip. Bremsstrahlung radiation from the rod tip irradiates extended objects meters distant from the source on the rod axis of symmetry. Success of the rod pinch derives from the small radiographic spot size for a range of driving voltages and x-ray spectra. In the present work, we examine two experimentally observed, and more subtle phenomena that may impact radiographic performance for some systems: flat-field nonuniformity in the image plane due to x-ray absorption in the rod, and weak, large-scale structures around radiographic features due to cathode-scattered x-rays.

Cathode-scattered x-rays have been observed in side-viewing pinhole images from a number of rod-pinch sources, including Cygnus and Gamble II, on which the rod pinch source was developed [1]. Also observed and studied here is a radial nonuniformity in flat-field images due to differential x-ray attenuation by the rod tip as a function of angle from the axis of symmetry. Measurements in a weakly-pinched, rod-pinch-like configuration on the HRS generator at NRL [3] show that the degree of nonuniformity is well-correlated with the axial extent of electron-beam deposition in the rod. X-ray imaging data from Cygnus [2] and HRS are analyzed by, and correlated with the ITS Monte-Carlo codes [4] to determine if the two phenomena considered here can impact radiographic performance in Cygnus. We believe that the present work represents the first systematic study of these rod-pinch-associated scattering and absorption effects.

*Work supported through Sandia National Laboratories, a multiprogram laboratory operated by Sandia Corporation, a Lockheed Martin Company, for the United States Department of Energy's National Nuclear Security Administration under contract DE-AC04-94AL85000.

[+]email: mosher@suzie.nrl.navy.mil

Report Documentation Page

Form Approved
OMB No. 0704-0188

1. REPORT DATE	2. REPORT TYPE	3. DATES COVERED
JUN 2009	**N/A**	**-**

4. TITLE AND SUBTITLE	5a. CONTRACT NUMBER
X-Ray Absorption And Scattering Issues For Rod-Pinch Radiographic Sources	5b. GRANT NUMBER
	5c. PROGRAM ELEMENT NUMBER
6. AUTHOR(S)	5d. PROJECT NUMBER
	5e. TASK NUMBER
	5f. WORK UNIT NUMBER
7. PERFORMING ORGANIZATION NAME(S) AND ADDRESS(ES) **Plasma Physics Division, Naval Research Lab., 4555 Overlook Ave. SW, Wash. DC 20375, USA**	8. PERFORMING ORGANIZATION REPORT NUMBER
9. SPONSORING/MONITORING AGENCY NAME(S) AND ADDRESS(ES)	10. SPONSOR/MONITOR'S ACRONYM(S)
	11. SPONSOR/MONITOR'S REPORT NUMBER(S)

12. DISTRIBUTION/AVAILABILITY STATEMENT
Approved for public release, distribution unlimited

13. SUPPLEMENTARY NOTES
See also ADM002371. 2013 IEEE Pulsed Power Conference, Digest of Technical Papers 1976-2013, and Abstracts of the 2013 IEEE International Conference on Plasma Science. IEEE International Pulsed Power Conference (19th). Held in San Francisco, CA on 16-21 June 2013., The original document contains color images.

14. ABSTRACT
During the past decade, the rod-pinch diode has been used extensively for high-brightness, megavolt x-ray radiography. Success of the rod pinch derives from its small radiographic spot size for a range of driving voltages and x-ray spectra. Here, we examine two experimentally observed and more subtle phenomena that may impact radiographic performance for some systems: flatfield nonuniformity in the image plane due to x-ray absorption in the rod, and weak, large-scale structures around radiographic features due to cathode-scattered xrays. X-ray imaging data from Cygnus and HRS are analyzed by the ITS Monte Carlo codes to determine if these phenomena are significant for Cygnus.

15. SUBJECT TERMS

16. SECURITY CLASSIFICATION OF:			17. LIMITATION OF ABSTRACT	18. NUMBER OF PAGES	19a. NAME OF RESPONSIBLE PERSON
a. REPORT	b. ABSTRACT	c. THIS PAGE			
unclassified	**unclassified**	**unclassified**	**SAR**	**6**	

II. FLAT-FIELD NONUNIFORMITY

The radial nonuniformity in flat-field images due to differential x-ray attenuation by the rod as a function of angle from the axis of symmetry was studied on the NRL HRS radiography source [3]. HRS is a 1-MV, 5-kA pulsed-power generator with a 1.6-mm-diam tapered tungsten rod anode. Because of the low current, the electron beam is not magnetically pinched onto the rod tip, and the axial distribution of electron deposition on the rod is determined only by electrostatic forces. A number of cathode configurations were studied, producing distributions with a variety of axial distributions.

Figure 1 shows an example of a side-viewing x-ray pinhole image of the HRS rod anode. The superimposed curve shows emission intensity vs axial position, acquired from a horizontal bandout of the image that covers the rod diameter. Similar bandouts taken above and below the rod were averaged and subtracted from the rod bandout in order to subtract background and artifacts due to pinhole blur on the tapered section. This net bandout is plotted in Fig. 1. The axial extent of electron deposition is defined as the 10%-to-10% width of the net bandout.

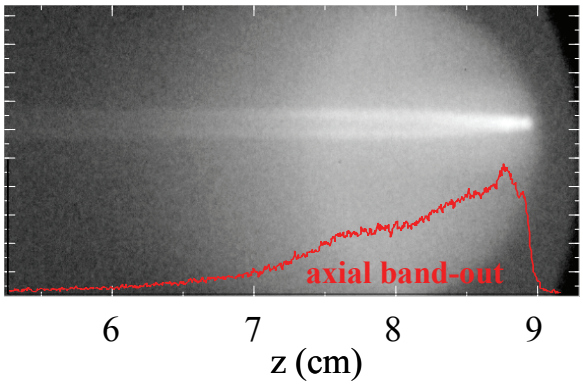

Figure 1. Side-viewing x-ray pinhole image of the HRS anode rod with its superimposed net axial bandout.

Figure 2 shows an example of the dose recorded by an on-axis image plate roughly 1 m from the source with an intervening 1-dimensional rolled edge. The image is in false color, ranging from blue for low dose to red for high dose. The width of the transition between the shadow of the rolled edge and the open flat-field region above it defines the radiographic spot size of the source. The sunrise-like radial distribution of dose in the open area is dose depression due to the reduced absorption path length of x-rays produced in the body of the rod with increased angle from the symmetry axis.

Figure 3 shows image plate vertical bandouts through the axis if symmetry for three HRS shots with different axial extents. The radiographic term for such a bandout perpendicular to the rolled edge is the edge spread function (ESF). The width in y of the sharply-increasing region is a measure of the radiographic spot size, while the open-region gradient is the differential-absorption

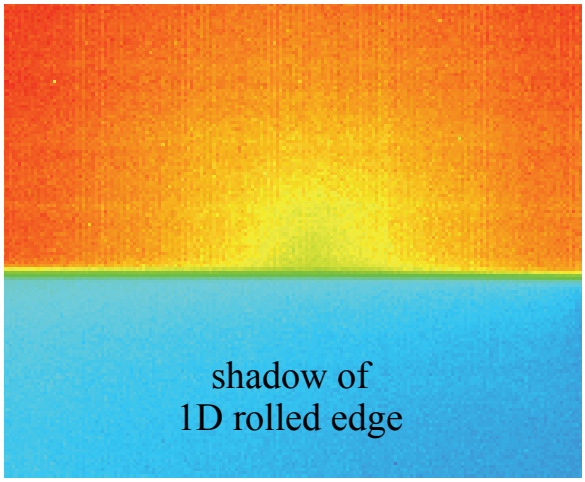

Figure 2. False color, on-axis image plate intensity for the HRS with a 1-dimensional rolled edge.

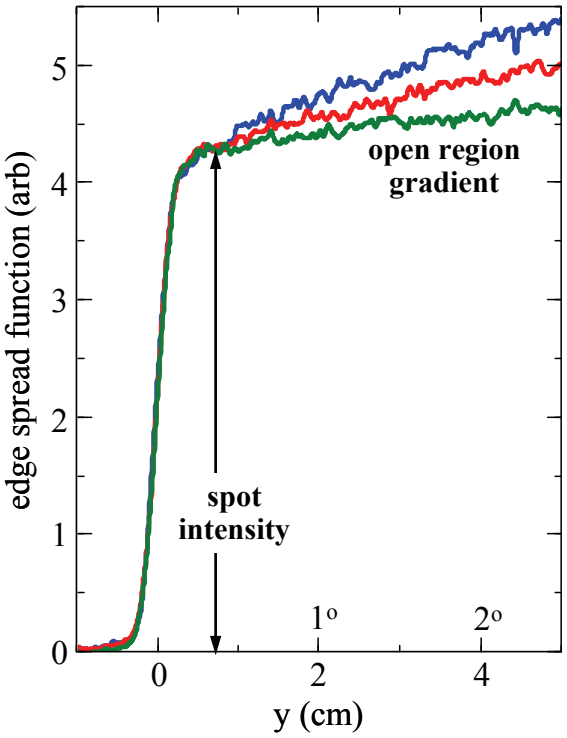

Figure 3. Vertical bandouts through the axis of symmetry for three HRS shots with different axial extents.

effect under study here. The secondary x-axis labels indicate the corresponding angle from the symmetry axis, and are used to define the slope in Fig. 4. Figure 4 plots the open-region slope normalized to spot intensity for 12 HRS shots with various axial extents, showing that the flat-field gradient is well correlated with the length over which the electron beam deposits in the rod. The three colored markers correspond to the matching color ESFs in Fig. 3. The least square fit to the markers is also shown.

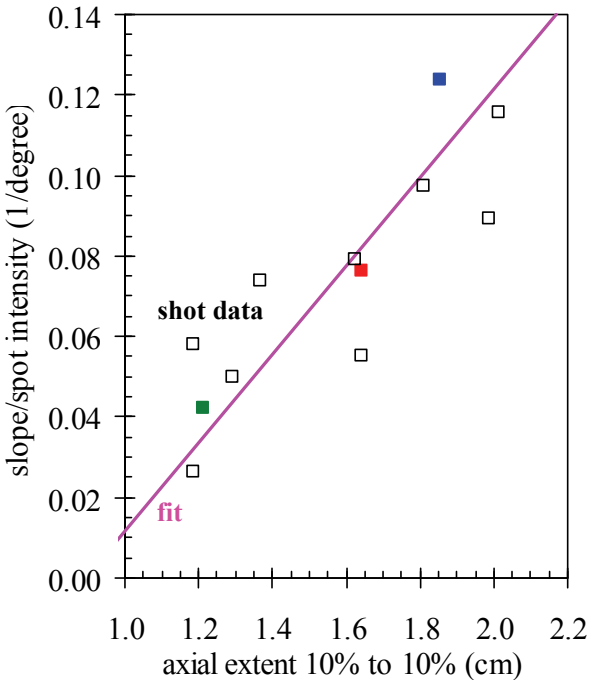

Figure 4. Open region slope normalized to spot intensity as a function of axial extent, and a least-squares fit.

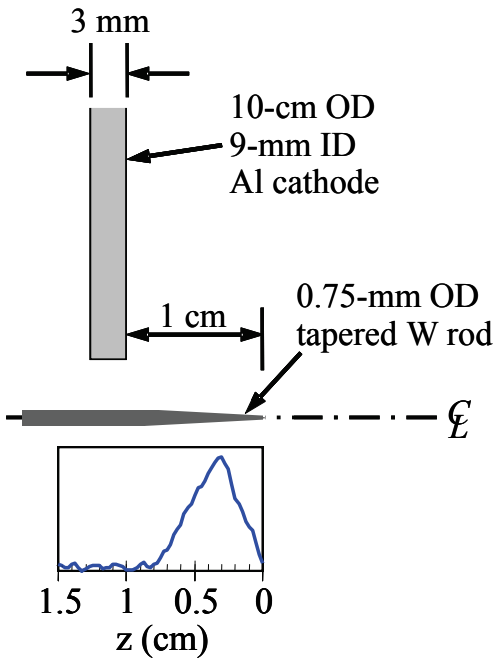

Figure 5. ITS configuration used to model the Cygnus rod pinch. The plot at the bottom shows the applied axial distribution of electron deposition in the rod.

Flat-field gradients due to differential absorption in the rod are expected to be much smaller for Cygnus than for HRS for a number of reasons. The Cygnus 0.75-mm rod diameter is about ½ that of HRS and, because of magnetic pinching of the electron beam, most emission is observed to be from the 5-mm-long taper to 0.25 mm at the rod tip. Additionally, the Cygnus x-ray spectrum is harder (> 2-MV bremsstrahlung rather than about 1 MV on HRS), so that it is less attenuated by the rod.

In order to quantify the size of open-field gradients from the Cygnus radiography source, its rod-pinch geometry, shown in Fig. 5, was modeled using the ITS Accept code [4]. Up to 10^9 electrons are injected into the rod normal to the symmetry axis with the axial distribution of electron deposition shown at the bottom of the figure. The axial distribution derives from the x-ray intensity vs z (axial line spread) derived from a side-viewing rolled edge. For the magnetically-pinched electron beam, deposition is concentrated in the tapered tip. The injected electron energy distribution, with about half of the electrons in the 2- to 2.3-MeV range, derives from the Cygnus voltage and current traces on the same shot (685) used to acquire the axial line spread. For the flat-field nonuniformity study, far-field x-ray spectra are collected in 0.5-degree azimuthal angle bins, and scattered radiation from the aluminum cathode is ignored.

Figure 6 shows the computed variation in recording phosphor dose as a function of angle from the axis of symmetry, acquired by post-processing the Accept spectra for thin (solid) and thick (dashed) aluminum transmission windows matched to thin and thick phosphors and three thicknesses of high-atomic-number filters (colors). The

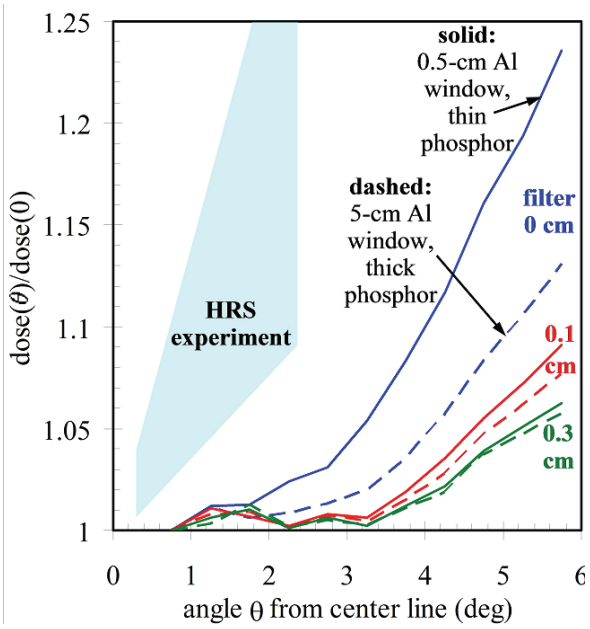

Figure 6. Computed variation of normalized phosphor dose as a function of angle from the axis of symmetry for thin (solid) and thick (dashed) aluminum transmission windows matched to thin and thick phosphors, and three thicknesses of high-atomic-number filters (colors).

dose is normalized to that calculated on the symmetry axis for each case. The statistical error for these computations is about 0.03 below 2 degrees, so that the results shown below this value are not significant. The Cygnus

image plane intercepts about 3 degrees about the axis of symmetry, so that only the softest spectrum (solid blue) has a significant, few-percent gradient across this field. Also shown in Fig. 6 is the range of gradients observed in the HRS experiments. Gradients observed on HRS are dramatically larger than those computed for Cygnus for the reasons indicated above.

III. CATHODE-SCATTERED X-RAYS

Figure 7 shows a side-viewing x-ray pinhole image of the Cygnus rod pinch and a matching drawing from the pinhole perspective. The overexposed pinhole image emphasizes the weak x-ray emission from the cathode. The drawing shows that the dim region in the center of the rod emission is due to x-ray absorption in the large-diameter cathode. Since any electrons impinging on the cathode must have energies close to zero, the cathode glow observed in rod pinches has been assumed to be due to x-rays from the rod being scattered in the cathode. In order to test this hypothesis, the Accept configuration of Fig. 5 has been used to model the Cygnus cathode glow and compare the predicted results to observation.

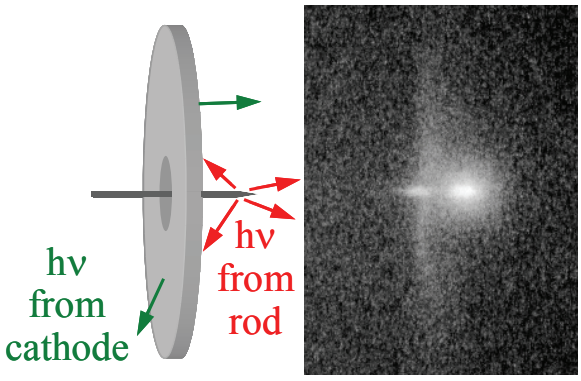

Figure 7. Side-viewing x-ray pinhole image of the Cygnus rod pinch and matching drawing from the pinhole perspective.

Figure 8 compares vertical bandouts (y direction on the Fig. 7 image) of the cathode glow from pinhole images on six Cygnus shots (colored) with the equivalent profile from ITS (black). The Cygnus bandouts are taken through the dim region of rod emission to minimize direct rod contributions. For the ITS profile, photons scattered from the cathode within 1 degree of the x axis (out of the page in Fig. 7) are added in 4-mm-wide Δy bins to simulate the glow viewed by the pinhole. This bin width is sufficient for reasonable photon counting statistics, but has insufficient resolution to reproduce the sharp experimental peak. Nevertheless, the agreement in measured and modeled shapes confirms that the cathode glow is due to scattered photons from the anode tip. The fall-off with y is due primarily to the inverse-square reduction of

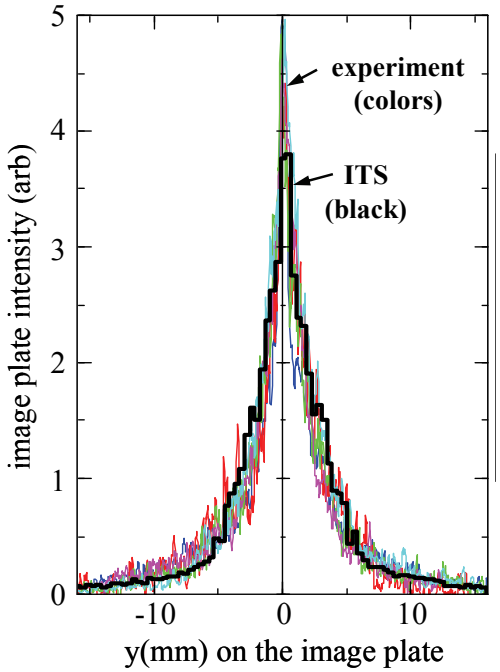

Figure 8. Vertical bandouts of the cathode glow from pinhole images on six Cygnus shots (colored) compared with the equivalent profile from ITS (black).

anode x-ray intensity at the cathode with distance from the rod tip.

Figure 9 compares the radial distributions of the rod and cathode-glow photon-number intensities from the ITS simulation. These distributions come from counting photons that cross the plane z = 0 (Fig. 5) in a 1-degree cone about the axis of symmetry and recording their crossing radii. The rod distribution goes to zero at the 0.375-mm rod radius. Rolled-edge-measured spot sizes are somewhat larger than this due to hydrodynamic expansion of the electron-heated rod-tip plasma [1, 5, 6], not included in the simulation. Based on the cathode radial profile of Fig. 9, assuming that the rod spot

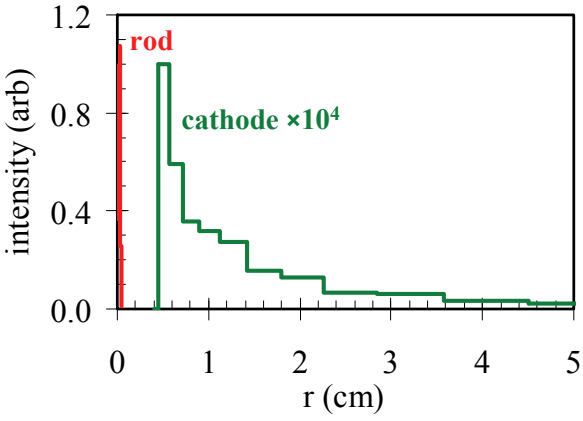

Figure 9. Radial distributions of the rod and cathode-glow x-ray intensities. The rod distribution goes to zero at the 0.375-mm rod radius.

(equivalent uniform disc) diameter is 1 mm, inclusion of the cathode glow formally increases the spot size by about 20%. This number is somewhat misleading because of the large area: the cathode-scattered x-radiation would produce extremely weak, likely unnoticeable, cm-sized halos around radiograph features that would probably not affect radiographic performance, and have image-plane intensities lower than the scattered x-ray background.

Figure 10 displays the photon number spectra (per steradian and incident electron) emitted by the rod and scattered from the cathode in the forward 3-degree cone subtended by the Cygnus image plane. The spectra have been attenuated by a 5-mm-thick aluminum transmission window in post-processing. Compared to the rod emission, the cathode emission shows down-scattering of the incident rod radiation (witness the shift in the tungsten K-line peak), and a fall off at high photon energies due to reduced scattering efficiency. The x-ray energy scattered by the glow into the 3-degree cone is calculated to be about 5% of that emitted by the rod into the same solid angle. Because of the low scattering efficiency of the aluminum cathode, this result seems counterintuitive. However, the cathode subtends about 1000-times greater solid angle of rod emission than the forward 3-degree cone, and the weak glow is emitted over about 7000-times the rod cross-sectional area.

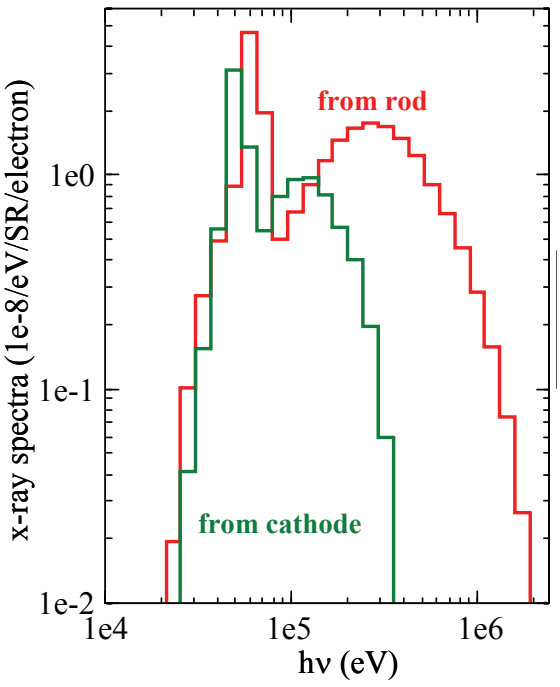

Figure 10. Photon number spectra per steradian and incident electron emitted by the Cygnus rod and scattered from the cathode in the forward 3-degree cone.

Cathode-scattered x-rays do not represent a serious concern for Cygnus radiography. Because of its soft spectrum and spatial separation from the rod, it can be effectively eliminated by collimation.

IV. CONCLUSIONS

Two absorption and scattering issues for rod-pinch radiography have been examined for their impact on radiographic systems. For a number of reasons, ITS results indicate that the substantial flat-field gradients observed on HRS due to differential rod absorption are not a concern for Cygnus. On HRS, the amplitude of the gradient is observed to be proportional to the axial length of rod over which electrons deposit (up to a few cm). For radiographic sources like HRS, where flat-field gradients are substantial, the gradients can distort radiographic images when changes in the object's x-ray contrast are gradual. The resulting smoothly-varying changes in image-plane dose may be distorted if they have length scales comparable to those of the flat-field gradients.

For Cygnus, most deposition is on the 5-mm taper, and the rod diameter is ½ that of HRS, so that the x-ray attenuation length is limited to several mm. Additionally, the Cygnus source spectrum is harder than that of HRS and is therefore less attenuated by the tungsten rod material. Also, hydrodynamic expansion of the rod tip on Cygnus [1, 5, 6] (not included in the present analysis), does not occur on the much weaker HRS. Expansion of the rod plasma by a radial factor A reduces the tungsten density by A^3 and increases the x-ray path length by A, reducing absorption by A^2, perhaps a factor-of-two effect for low-energy photons on Cygnus. This phenomenon was observed in step-wedge measurements carried out in NRL Gamble II plasma-filled rod-pinch experiments, where the observed soft spectral region was enhanced over ITS predictions that assumed a solid-density rod [7].

The spatial distribution of the cathode x-ray glow computed with ITS matches those observed in Cygnus side-viewing x-ray pinhole images. ITS results also indicate that the forward-scattered photons from the cathode can be effectively eliminated by collimation, a fixture of the Cygnus experiments. Even for rod-pinch sources without collimation, the cathode-scattered x-radiation would produce extremely weak, cm-sized halos around radiograph features that would be unlikely to affect radiographic performance. With cathode-scattered radial intensities down from those from the rod-pinch by about 10^4, their contribution to image-plane dose will probably be much lower than those due to the scattered x-ray background.

V. REFERENCES

[1] G. Cooperstein, J.R. Boller, R.J. Commisso, D.D. Hinshelwood, D. Mosher, P.F. Ottinger, J.W. Schumer, S.J. Stephanakis, S.B. Swanekamp, B.V. Weber, and F.C. Young, "Theoretical Modeling and Experimental Characterization of a Rod-Pinch Diode," Phys. Plasmas, vol. 8, p. 4618, 2001.

[2] B.V. Oliver, G. Cooperstein, S.R. Cordova, D. Crain, D. Droemer, T. Haines, D. Hinshelwood, N. King, S. Lutz, C.L. Miller, I. Molina, D. Mosher, D. Nelson, E. Ormond, S. Portillo, J. Smith, D. Welch, and W.M. Wood, these Proceedings, paper 01-1 (Invited).

[3] R.J. Allen, G. Cooperstein, F.C. Young, J.W. Schumer, D.D. Hinshelwood, D. Mosher, D. Holmberg, and S.E. Mitchell, "Characterization and Optimization of a Compact 1-MV, 6-kA Radiographic Source," in Proc. 14th IEEE International Pulsed Power Conf., 2003, p. 883.

[4] J.A. Halbleib, R.P. Kensek, G.D. Valdez, S.M. Seltzer, and M.J. Berger, "ITS: The Integrated TIGER Series of electron/photon transport codes-Version 3.0," IEEE Trans. Nucl. Sci., vol. 39, p. 1025, 1992.

[5] D. Mosher, J.W. Schumer, D.D. Hinshelwood, B.V. Weber, S.J. Stephanakis, S.B. Swanekamp, and F.C. Young, "An Electron-Beam-Heating Model for the Gamble II Rod Pinch," in Proc. 14th International Conf. on High-Power Particle Beams, 2002, p. 199.

[6] S. Portillo, S.S. Lutz, L.P. Mix, K. Hahn, D. Rovang, J.E. Maenchen, I. Molina, S. Cordova, D. Droemer, R. Chavez, and D. Ziska, "Time-Resolved Spot Size Measurements from Various Radiographic Diodes on the RITS-3 Accelerator," IEEE Trans. Plasma Sci., vol 34, p. 1908, 2006.

[7] B.V. Weber, R.J. Allen, R.J. Commisso, G. Cooperstein, D.D. Hinshelwood, D. Mosher, D.P. Murphy, P.F. Ottinger, D.G. Phipps, J.W. Schumer, S.J. Stephanakis, S.B. Swanekamp, S. Pope, J. Threadgold, L. Biddle, S. Clough, A. Jones, M. Sinclair, D. Swatton, and T. Carden, "Radiographic Properties of Plasma-Filled Rod-Pinch Diodes," IEEE Trans. Plasma Sci., vol 36, p. 443, 2008.